

# Devil's staircase in a nanotube

Dmitry S. Novikov\*

Department of Electrical Engineering and Department of Physics, Princeton University, Princeton, NJ 08544

(Dated: December 2, 2024)

Nanotube electrons in a periodic potential form a devil's staircase of incompressible states. Excitation gaps are obtained via the phase soliton method developed for the four fermion modes. In the semi-classical limit of the strong electron interactions, the effective description in terms of spinless Dirac fermions follows from the saddle point of the bosonized action for the charge and spin modes, and subsequent re-fermionization. Incompressible states can be detected in a Thouless pump setup, in which a slowly moving periodic potential induces quantized current, with a possibility to pump on average a fraction of an electron per cycle.

PACS numbers: 71.10.Pm, 85.35.Kt, 64.70.Rh

In the present work we propose coupling of the nanotube (NT) electrons to an external periodic potential as a means to study and detect Wigner crystallization [1] via commensuration. [2] We show that incompressible electron states arise when the NT electron number density  $\bar{\rho}$  (counted from half-filling) is commensurate with the potential period:

$$\bar{\rho} = m_{\text{tot}}/\lambda_{\text{ext}} , \quad m_{\text{tot}} = 4m . \quad (1)$$

In Eq. (1),  $m$  is the number of NT fermions of each of the four polarizations [3] per potential period  $\lambda_{\text{ext}}$ . We generalize the Pokrovsky–Talapov theory [2] for the case of the four modes, and calculate excitation gaps.

In the absence of interactions, Bragg diffraction opens minigaps at integer density (1),  $|m| = 1, 2, \dots$ . [4] Interactions dramatically change the spectrum, resulting in a devil's staircase of incompressible states at any *ratio*nal  $m = p/q$ . Semiclassically, in such a state, the NT electron system is locked by the potential into a  $q\lambda_{\text{ext}}$ –periodic structure. If detected, *e.g.* in a Thouless pump setup [4], corresponding minigaps would provide a direct probe of interactions, with a possibility to map the devil's staircase by pumping at fractions of the base frequency.

One-dimensional interacting electrons are conventionally described by the Tomonaga–Luttinger liquid. [5] This hydrodynamic approach is valid in a small momentum shell near the Fermi points, when excitations are delocalized. Adequate description of crystallization and commensurability requires including the *curvature* of the electronic dispersion that becomes important at low density. The curvature can yield crystallization or commensuration by coupling charge and spin modes and by introducing a *length scale* into an otherwise scale–invariant Gaussian theory. In this work we treat both electron interactions and the curvature of the dispersion non-perturbatively by making use of the relativistic Dirac spectrum of a half-filled nanotube. Curvature is controlled by the Dirac gap and is bosonized exactly by virtue of the massive Thirring — sine–Gordon duality. [6, 7] This enables us to study incompressible states both in the limit of a narrow-gap Luttinger liquid and that of

the locked Wigner crystal.

Our course of action is to introduce the bosonized description for the NT electrons, develop the phase soliton method and find excitation gaps from the renormalized sine–Gordon action, draw the phase diagram in the semi-classical limit, and comment on the experimental means to detect incompressible states.

*The model.*— Nanotube electrons in the forward scattering approximation [8] are described by the four flavors of Dirac fermions  $\psi_{\alpha} = (\psi_{\alpha}^R \psi_{\alpha}^L)^T$ ,  $\alpha = 1–4$ , whose interaction is written in terms of the smooth envelope  $\rho(x) = \sum_{\alpha=1}^4 \psi_{\alpha}^+(x)\psi_{\alpha}(x)$  of the total charge density. The Hamiltonian in the second–quantized form is

$$\mathcal{H} = \mathcal{H}_0 + \mathcal{H}_{\text{bs}} + \mathcal{H}_{\text{ext}} . \quad (2)$$

The first term  $\mathcal{H}_0$  is the massless Dirac Hamiltonian

$$\mathcal{H}_0 = -i\hbar v \int \sum_{\alpha=1}^4 \psi_{\alpha}^+ \sigma_3 \partial_x \psi_{\alpha} dx + \frac{1}{2} \sum_k \rho_{-k} V(k) \rho_k \quad (3)$$

with the Coulomb interaction  $V(k) = \frac{2e^2}{\varepsilon+1} \ln [1 + (ka)^{-2}]$  for a tube of radius  $a$  placed on a substrate with the dielectric constant  $\varepsilon$ . The curvature of the electron dispersion controlled by the gap  $2\Delta_0$  at half-filling introduces backscattering at each NT Dirac point:

$$\mathcal{H}_{\text{bs}} = \Delta_0 \int \sum_{\alpha=1}^4 \psi_{\alpha}^+ \sigma_1 \psi_{\alpha} dx . \quad (4)$$

We emphasize that the backscattering  $\Delta_0$  is *not* the usual interaction–induced  $V(2k_F)$ –term (which is undetectably small in metallic NTs), but rather is present at the single-particle level [3, 9]: Depending on the tube chirality, the bare gap  $\Delta_0$  can be in the range  $\Delta_0 \lesssim 10$  meV to  $\sim 0.5$  eV; it can also be controlled by the parallel magnetic field. [10] Adding periodic potential  $U(x)$  and the chemical potential  $\mu$  [ $\mu = 0$  at half-filling] results in

$$\mathcal{H}_{\text{ext}} = \int dx \rho(x) \{U(x) - \mu\} , \quad (5)$$

$$U(x) = A \cos k_{\text{ext}} x , \quad k_{\text{ext}} = 2\pi/\lambda_{\text{ext}} . \quad (6)$$

Qualitatively, our findings will be valid for any realistic potential which justifies the simplest choice (6); typically,  $\lambda_{\text{ext}} \sim 0.1 - 1 \mu\text{m}$ . The Hamiltonian (2) is U(4)-invariant with respect to rotations in the fermion flavor space.

Bosonization of the nanotube electrons  $\psi_\alpha = \frac{1}{\sqrt{2\pi a}} e^{i\Theta_\alpha}$  is exact even in the presence of (4). It maps the problem of the four modes of interacting Dirac fermions onto the sine-Gordon model of the four interacting boson fields  $\Theta_\alpha$ . We rotate [4, 11] to the basis of the charge mode  $\theta^0$  and three neutral modes  $\theta^a$ , in which case the charge density  $\rho(x) = \frac{2}{\pi} \partial_x \theta^0$ , and the Gaussian action (bosonized  $\mathcal{H}_0$ ) is diagonal [ $\hbar = v = 1$ ]:

$$\mathcal{L}_0 = \frac{1}{2\pi} \int dx \left( (\partial_t \theta^0)^2 - K (\partial_x \theta^0)^2 + \sum_{a=1}^3 (\partial_\mu \theta^a)^2 \right). \quad (7)$$

The slow momentum dependence of the charge stiffness  $K_k = 1 + 4\nu V(k)$ ,  $\nu^{-1} = \pi\hbar v$ , is irrelevant, and we take it as constant  $K \equiv K_{k \sim 1/l_{\text{ch}}}$ ,  $l_{\text{ch}}$  being the size of the charged-mode soliton (described below). Assuming  $l_{\text{ch}} \sim l_s$ , with the screening length  $l_s \sim 1 \mu\text{m}$ , and using  $e^2/\hbar v \simeq 2.7$ , one estimates  $K \simeq 40$  for the stand-alone tube;  $K \simeq 10$  if the tube is placed on a substrate with dielectric constant  $\varepsilon \simeq 10$ . The logarithmic behavior of  $V(k)$  underlies the fact that the Coulomb interaction is essentially *local* in one dimension,  $\frac{e^2}{2} \int dx dx' \rho(x) \rho(x')/|x - x'| \simeq \frac{\hbar v}{2\pi} \int dx K (\partial_x \theta^0)^2$ .

The nonlinear part of the sine-Gordon Lagrangian [coming from  $\mathcal{H}_{\text{bs}}$ ] reads [4, 11, 12]

$$\mathcal{L}_{\text{bs}} = - \int dx g_0 \mathcal{F} \left( \theta^0 + 2\tilde{\mu} k_{\text{ext}} x - 2\tilde{A} \sin k_{\text{ext}} x, \theta^a \right), \quad (8)$$

$$\mathcal{F}(\theta^0, \theta^a) = \cos \theta^0 \cdot \prod_{a=1}^3 \cos \theta^a + \sin \theta^0 \cdot \prod_{a=1}^3 \sin \theta^a, \quad (9)$$

where  $g_0 = 4\Delta_0/\pi D a^2$ , and  $D \simeq \hbar v/a$  is the 1d bandwidth. In Eq. (8) we included the coupling (5) to external fields by shifting the charge mode  $\theta^0 \rightarrow \theta^0 - \frac{2}{\hbar v} \int^x K^{-1}(U - \mu) dx'$ , with  $\tilde{\mu} = \mu/K\hbar k_{\text{ext}} v$ ,  $\tilde{A} = A/K\hbar k_{\text{ext}} v$ .

In what follows, it is useful to first describe elementary excitations of the stand-alone tube,  $U \equiv 0$ . As shown by Levitov and Tsvelik [11], in the bosonized language adding one electron corresponds to a *composite soliton* of both the charge and the flavor modes. In such a composite object, the charge mode changes by  $\pi/2$  (adding charge 1) over the length  $l_{\text{ch}}$ , whereas the neutral sector adds a particular SU(4) flavor to the electron by means of the solitons of  $\theta^a$  “switching” by  $\pm\pi/2$  on a shorter scale  $l_{\text{fl}} \sim K^{-1/2} l_{\text{ch}}$ , right in the middle of the charge soliton. The composite soliton is a charge 1 configuration of the minimal energy, obtained by optimizing the action  $\mathcal{L}_0 + \mathcal{L}_{\text{bs}}$  in the limit of large Coulomb repulsion  $K \gg 1$ . Technically, such an optimization results in the soft neutral modes  $\theta^a$  adjusting to create the effective potential  $\bar{\mathcal{F}}(\theta^0) = \min_{\{\theta^a\}} \mathcal{F}(\theta^a, \theta^0) \sim \cos 4\theta^0$  for the stiff charge mode  $\theta^0$ .

In the absence of external potential,  $U \equiv 0$ , the system  $\mathcal{L}_0 + \mathcal{L}_{\text{bs}}$  describes the Wigner crystal — Luttinger liquid crossover. In particular, raising the chemical potential from half-filling [band insulator, or the “Dirac vacuum”] to just above the charge gap produces the train of weakly-overlapping composite solitons described above [ $\bar{\rho}l_{\text{fl}} \ll 1$ , “Wigner crystal”], in which overlapping charge solitons ( $\bar{\rho}l_{\text{ch}} > 1$ ) maintain a quasi-long-range order. Further increase of  $\mu$  leads to strongly overlapping solitons rendering the nonlinear term (8) irrelevant [ $\bar{\rho}l_{\text{fl}} \gg 1$ , Luttinger liquid]. We emphasize that the crystal—liquid crossover occurs due to the *finite* soliton size  $l_{\text{fl}} \propto \Delta_0^{-\zeta}$  that scales inversely with the curvature of the dispersion. Curvature is also responsible for binding flavor with charge through the term (8). The  $U \equiv 0$  system is compressible. [11]

Periodic potential locks electrons into incompressible states. Technically, the term (8) becomes relevant whenever the density  $2\tilde{\mu} = m$  [Eq. (1)] is integer. [4] When  $m$  is a simple fraction,  $2\tilde{\mu} = p/q$ , to identify incompressible states one utilizes the phase soliton method. [2] We generalize it for the case of the four nanotube modes by expanding in powers of the coupling  $g_0$  as  $\theta^j = \bar{\theta}^j + g_0 \theta^{j(1)} + \dots + g_0^n \theta^{j(n)} + \dots$ ,  $j = 0, a$ , and finding the effective Lagrangian  $\mathcal{L}_m[\bar{\theta}^0, \bar{\theta}^a]$  for the *phase* modes  $\bar{\theta}^0$  and  $\bar{\theta}^a$ ,  $a = 1 - 3$ , to the lowest order in  $g_0$ . The phase modes  $\bar{\theta}^0, \bar{\theta}^a$  are constant in the commensurate phase, whereas an excitation is a *composite phase soliton*, in which the phase fields  $\bar{\theta}^0(x), \bar{\theta}^a(x)$  describe a slow deformation of the regular commensurate configuration. Excitation gap is given by the energy of the composite soliton, renormalized by quantum fluctuations.

We underline that it is the curvature  $\propto \Delta_0$  that causes commensuration. Same is true for the non-interacting electrons: When  $\Delta_0 = 0$ , the external potential is gauged away from the Hamiltonian  $-i\hbar v \sigma_3 \partial_x + U(x)$ .

The composite phase soliton is a result of optimization of the corresponding effective action  $\mathcal{L}_m[\bar{\theta}^0, \bar{\theta}^a]$  (examples of which are given below). This problem will be similar to the  $U \equiv 0$  case described above: When interaction is strong,  $K \gg 1$ , the neutral phase modes  $\bar{\theta}^a$  adjust [on the scale  $\bar{l}_{\text{fl}}$ ] to create an effective potential for the charged phase mode  $\bar{\theta}^0$ . The crucial difference from the former case is that this optimization will qualitatively depend on whether the system is in the regime of Luttinger liquid or that of the Wigner crystal. In this sense, periodic potential naturally distinguishes between the opposite sides of the crystal—liquid crossover, by bringing about the additional *length scale*, its period  $\lambda_{\text{ext}}$ . Technically, the saddle point of  $\mathcal{L}_m$  will depend on whether the neutral modes are adiabatic or fast on the length scale on which the effective potential (8) changes appreciably. Below we consider both cases separately.

*Bragg diffraction in a four-flavor Luttinger liquid.* — In the adiabatic limit,  $\bar{l}_{\text{fl}} \gg \lambda_{\text{ext}}$ , the flavor excitation

is delocalized, which results in importance of *exchange*: The system (correlated over many  $\lambda_{\text{ext}}$ ) “knows” that it is comprised of particles of four different flavors. This limit is connected to the non-interacting case, where particles repel only due to the Pauli principle. For integer density  $m$ , averaging (8) over the period  $\lambda_{\text{ext}}$  reduces the problem to the  $U \equiv 0$  case with  $\mathcal{L}_m = \mathcal{L}_0 + \mathcal{L}_{\text{bs}}$ ,  $g_0 \rightarrow g_0 J_m(2\tilde{A})$ , yielding the  $K \gg 1$  minigaps  $\Delta_m \simeq K^{1/2} D^{1/5} |\Delta_m^{(0)}|^{4/5}$  that are enhanced by the quantum fluctuations compared to the noninteracting values  $\Delta_m^{(0)} = 2\Delta_0 J_m(2\tilde{A})$ . [4]

The fractional  $m = 1/2$  case is considered in detail in Ref. 12. A somewhat lengthy calculation yields the effective action of the form  $\mathcal{L}_{1/2} = \mathcal{L}_0 + v(\tilde{A}) \sum_a \cos 2\bar{\theta}^0 \cos 2\bar{\theta}^a - u(\tilde{A}) \sum_{a>b} \cos 2\bar{\theta}^a \cos 2\bar{\theta}^b$ . We find the *charge* excitation gap  $\Delta_{1/2} \propto \frac{K-1}{\sqrt{K}} D \left( \frac{\Delta_0}{\epsilon_0} \right)^2$  (that vanishes in the noninteracting limit  $K \rightarrow 1$  in accord with the Bloch theory), whereas *flavor* excitations are governed by the  $\text{SU}(4) \simeq \text{O}(6)$  Gross–Neveu Lagrangian [13] that can be written in terms of six Majorana fermions  $\chi \sim e^{i\theta}$ ,  $\mathcal{L}_{\text{GN}} = i\bar{\chi}_j \gamma_\mu \partial_\mu \chi_j - u(\tilde{A})(\bar{\chi}_j \chi_j)(\bar{\chi}_{j'} \chi_{j'})$ . Although the charge gap  $\Delta_{1/2}$  vanishes for certain values of the potential amplitude (zeroes of  $v(\tilde{A})$  given in Ref. 12), the excitation gap never vanishes due to flavor, since the Gross–Neveu coupling  $u(\tilde{A}) \neq 0$ .

*Locked Wigner crystal.*— In the remainder of this work we focus on the opposite limit  $\bar{l}_{\text{fl}} \ll \lambda_{\text{ext}}$ , in which the physics is dominated by the charge mode, whereas exchange (overlap of the flavor solitons) is relatively unimportant. Below we show that the effective description in

this regime is that of a *single* mode of fermions with the density (1), locked by the external potential. Physically this happens since when electron wavefunctions (represented by solitons) are *localized*, Coulomb repulsion wins over exchange. Naturally, in this case the appropriate saddle point of  $\mathcal{L}_0 + \mathcal{L}_{\text{bs}}$  gives the semi-classical description, with the WKB condition  $\bar{l}_{\text{fl}} \ll \lambda_{\text{ext}}$ . Technically, the neutral mode “switching” produces the effective charge mode potential with a quarter-period, similarly to the  $U \equiv 0$  case above:  $g_0 \mathcal{F}(\theta^0 + m_{\text{tot}} k_{\text{ext}} x - 2\tilde{A} \sin k_{\text{ext}} x, \theta^a) \sim g \cos(4\theta^0 + m_{\text{tot}} k_{\text{ext}} x - 8\tilde{A} \sin k_{\text{ext}} x)$ . This potential now depends on the *total density*  $m_{\text{tot}}$ , Eq. (1).

To obtain the renormalized coupling  $g$  we utilize adiabaticity of  $U(x)$ ,  $\bar{l}_{\text{fl}} \ll \lambda_{\text{ext}}$ . The renormalization group produces the effective coupling  $g$  on the scales  $a < l < l_{\text{fl}}$  that appear “microscopic” for the external potential. Thus the neutral modes can be integrated out, yielding both  $l_{\text{fl}}$  and  $g$  independent of the shape of the potential  $U(x)$ . The problem becomes similar to the  $U \equiv 0$  case. The coupling  $g$  follows from the scaling  $g \simeq g_0 (l_{\text{fl}}/a)^{-3/4}$  and self-consistency  $g(l_{\text{fl}}) \sim 1/l_{\text{fl}}^2$ . [4, 11, 12]

*Re-fermionization.*— Let us now complete our single-mode description by mapping the system in the limit  $\bar{l}_{\text{fl}} \ll \lambda_{\text{ext}}$  onto the problem of spinless Dirac fermions in the external potential (6). We introduce the displacement field  $\Theta = 2\theta^0$  for the total density  $\rho \equiv \frac{1}{\pi} \partial_x \Theta$ . To preserve commutation relations, we rescale the canonical momentum  $\Pi_\Theta = \frac{1}{2} \Pi_{\theta^0}$ . Changing variables in the Lagrangian  $\frac{1}{2\pi} \{ K(\partial_x \theta^0)^2 + g \cos(4\theta^0 + \dots) \}$ , we obtain the effective Lagrangian for the single mode  $\Theta$ ,

$$\mathcal{L}_{\text{eff}}[\Theta] = \frac{\hbar v'}{\pi} \int dx \left\{ \frac{1}{2v'^2} (\partial_t \Theta)^2 - \frac{K'}{2} (\partial_x \Theta)^2 - g \cos(2\Theta + m_{\text{tot}} k_{\text{ext}} x - 2\tilde{A}' \sin k_{\text{ext}} x) \right\} \quad (10)$$

with rescaled parameters  $v' \equiv 4v$ ,  $K' \equiv K/16$ , and  $\tilde{A}' \equiv A/K' \hbar k_{\text{ext}} v' = 4\tilde{A}$ . The velocity quadrupling corresponds to counting incoming fermions regardless of their (four) flavors. With the same accuracy that allowed us to neglect the flavor sector, the rescaled value  $K' \approx 1 + (K-1)/16 \equiv 1 + \nu' V(q)$  is by definition the charge stiffness for the spinless Dirac fermions of velocity  $v'$ , with the density of states  $\nu' = 1/\pi \hbar v'$ . The external fields  $U$  and  $\mu$  are not rescaled. Introducing the Dirac spinors  $\Psi = \frac{1}{\sqrt{2\pi a'}} e^{i\Theta}$  relative to the new cutoff  $a' \sim l_{\text{fl}}$ , we obtain the effective Hamiltonian

$$\mathcal{H}_{\text{eff}}[\Psi] = \int dx \Psi^+ \{ -i\hbar v' \sigma_3 \partial_x + \Delta' \sigma_1 + U(x) - \mu \} \Psi + \frac{1}{2} \sum_k \rho_{-k} V(k) \rho_k \quad (11)$$

for the fictitious spinless Dirac fermions of charge  $e$ , with the number density  $\rho(x) = \Psi^+ \Psi$ , coupled to the external fields in the natural way, Eq. (5). The effective gap  $\Delta'$  in Eq. (11) is chosen in such a way that it corresponds to the renormalized coupling  $g$  entering the Lagrangian (10),  $g \simeq \frac{\Delta'}{\hbar v' a'}$ , yielding  $\Delta' \simeq \frac{\hbar v'}{l_{\text{fl}}} \simeq D^{1/5} \Delta_0^{4/5}$ . The (charge) excitation gaps are now estimated by utilizing

the phase soliton approach [2] for the single mode system (10),(11) yielding the devil’s staircase. For integer  $m_{\text{tot}} = \pm 1, \pm 2, \dots$ , in the classical limit  $K \rightarrow \infty$ , we find

$$\Delta_m \simeq K^{1/2} |J_{m_{\text{tot}}}(2\tilde{A}')|^{1/2} D^{1/5} \Delta_0^{4/5}. \quad (12)$$

The effective density quadrupling  $m \rightarrow m_{\text{tot}}$  in (12) is due to strong interactions: Electrons of all flavors avoid

each other, their ground state being a Slater determinant of the quadrupled size.

*Phase diagram.*— Coarse-graining beyond  $l_{\text{fl}}$ , in the limit  $K \gg 1$ , we treat fermions as classical point electrons (with positions  $x_i$ ) and holes ( $y_j$ ) that interact with each other via the Coulomb potential, their classical energy

$$E_{\text{cl}} = \sum_{i=1..N_e} (\Delta' + U(x_i)) + \sum_{j=1..N_h} (\Delta' - U(y_j)) + \sum_{\substack{i,j=1 \\ i>j}}^N \frac{e^2}{|x_i - x_j|} + \sum_{\substack{i,j=1 \\ i>j}}^N \frac{e^2}{|y_i - y_j|} - \sum_{\substack{i,j=1 \\ i>j}}^N \frac{e^2}{|x_i - y_j|}. \quad (13)$$

Here  $N_e$  and  $N_h$  are the total number of electrons and holes in correspondingly the minima and maxima of  $U(x)$ . Minimizing  $E_{\text{cl}}(A) - \mu(N_e - N_h)$ , one obtains the characteristic Coulomb blockade hexagons, Fig. 1(a), their size controlled by the NT capacitance per period,  $C_0 = \frac{\lambda_{\text{ext}}}{2 \ln(l_s/\lambda_{\text{ext}})}$ . We label the domains by the pairs  $(n_e, n_h)$  of electron and hole numbers per period. At large  $n_e, n_h \gg 1$ , approximating the density  $\rho(x)$  by the continuous function  $\rho_{\text{TF}}(x) \propto U(x)$ , we estimate interaction energy inside each half-period (“quantum dot”) as  $\frac{e^2}{2} \int dx dx' \frac{\rho_{\text{TF}}(x)\rho_{\text{TF}}(x')}{|x-x'|} \equiv \frac{n_e^2 e^2}{2C_1}$ , where the “dot capacitance”  $C_1 \simeq \frac{\lambda_{\text{ext}}}{2\pi \ln(\lambda_{\text{ext}}/l_{\text{fl}})}$ . In this limit, all the honeycomb regions of the phase diagram become identical with their period in  $A$  being  $e^2/C_1$ . Remarkably, this period exactly follows from Eq. (12) with  $\tilde{A}' \approx \frac{\pi}{2} \cdot \frac{A}{e^2/C_1}$  [ $K \equiv K_1/\lambda_{\text{ext}} \approx K - 1$ ], using Bessel functions zeroes  $2\tilde{A}'_{m_{\text{tot}}}^{(s)} \simeq \text{const} + \frac{\pi m_{\text{tot}}}{2} + \pi s$ ,  $s = \min\{n_e, n_h\}$ . The borders between the domains correspond to the incompressible states with *fractional*  $n_e$  and  $n_h$  (not shown).

*Quantized current.*— The devil’s staircase can be mapped in the Thouless pump setup. [4] With the chemical potential inside the gap, adiabatically moving wave  $U(x - st)$  with frequency  $f = s/\lambda_{\text{ext}}$  will generate quantized current  $j = m_{\text{tot}} e f$ . The moving potential can be created by gating, optical methods, or acoustic field. Novel incompressible states with fractional  $m$  would cor-

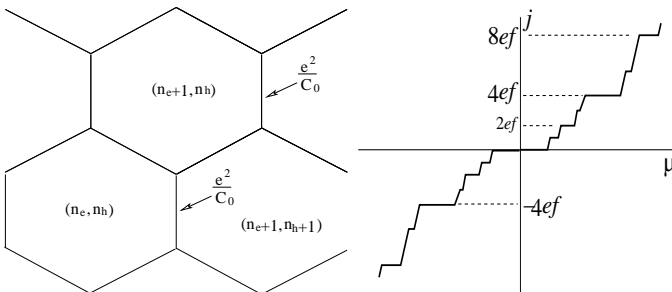


FIG. 1: (a) Phase diagram in the  $(A, \mu)$  plane according to the model (13). In the limit  $n_e, n_h \gg 1$  all the regions of the phase diagram are identical, with their period in  $A$  given by  $e^2/C_1$ . (b) Mapping the devil’s staircase in the Thouless pump setup. In addition to the integer- $m$  plateaus, the ones with fractional  $m$  appear due to electron interactions.

respond to the current quantized in the *fractions* of  $4ef$ , as schematically shown in Fig. 1(b). Current changes sign at half-filling due to the Dirac nature of the NT.

*Conclusions.*— We demonstrated that coupling of nanotube electrons to a periodic potential results in the devil’s staircase of incompressible states. Excitation gaps are found both in the limit of narrow-gap Luttinger liquid, and in the semi-classical Wigner crystal regime, by selecting the saddle point of the nonlinear action of the four bosonic modes. When the Coulomb interaction dominates, the system behaves as a single Dirac fermion mode with renormalized mass and velocity. Control over the nanotube gap and the periodic potential makes the adiabatic pumping setup [4] a unique probe of the Luttinger liquid—Wigner crystal crossover, of the electron interactions, and commensurability effects in 1d. Novel effect of pumping at fractions of base frequency is linked to the existence of interaction-induced incompressible states. Applied to the Coulomb drag problem, [14] the developed approach yields the devil’s staircase of the absolute drag states. The effective single-mode description could also rationalize recent manifestations of Wigner crystallization in transport, such as  $e^2/h$  steps in conductance. [15]

This work was supported by NSF MRSEC grant DMR 02-13706.

\* Electronic address: [dima@alum.mit.edu](mailto:dima@alum.mit.edu)

- [1] L.I. Glazman, I.M. Ruzin, and B.I. Shklovskii, Phys. Rev. B **45**, 8454 (1992); H.J. Schulz, Phys. Rev. Lett. **71**, 1864 (1993); S. Capponi, D. Poilblanc, T. Giamarchi, Phys. Rev. B **61**, 13410 (2000)
- [2] V.L. Pokrovsky, A.L. Talapov, Sov. Phys. JETP **75**, 1151 (1978); P. Bak, Rep. Prog. Phys. **45**, 587 (1982); J. Frenkel and T.A. Kontorova, Zh. Eksp. Teor. Fiz. **8**, 1340 (1938)
- [3] R. Saito, G. Dresselhaus and M. S. Dresselhaus, *Physical Properties of Carbon Nanotubes*, Imperial College Press, London, 1998.
- [4] V.I. Talyanskii, D.S. Novikov, B.D. Simons, L.S. Levitov, Phys. Rev. Lett. **87**, 276802 (2001); [cond-mat/0105220](http://arxiv.org/abs/cond-mat/0105220)
- [5] M. Stone (Ed.), *Bosonization*, World Scientific, Singapore (1994)
- [6] S. Coleman, Phys. Rev. D **11**, 2088 (1975)
- [7] F.D.M. Haldane, J. Phys. A **15**, 507 (1982)
- [8] Y.A. Krotov, D.-H. Lee, S.G. Louie, Phys. Rev. Lett. **78**, 4245 (1997); R. Egger, A. O. Gogolin, Phys. Rev. Lett. **79**, 5082 (1997); C. Kane, L. Balents, M. P. A. Fisher, Phys. Rev. Lett. **79**, 5086 (1997); A. Odintsov and H. Yoshioka, Phys. Rev. Lett. **82**, 374 (1999)
- [9] C. L. Kane and E. J. Mele, Phys. Rev. Lett. **78**, 1932 (1997); C. Zhou, J. Kong, and H. Dai, Phys. Rev. Lett. **84**, 5604 (2000); M. Ouyang, J.L. Huang, C.L. Cheung, C.M. Lieber, Science **292**, 5517 (2001)
- [10] H. Ajiki and T. Ando, J. Phys. Soc. Jpn. **65**, 505 (1996); J.-O. Lee, J. R. Kim, J. J. Kim, J. Kim, N. Kim, J. W. Park, and K. H. Yoo, Sol. Stat. Comm. **115**, 467 (2000); U.C. Coskun, T.-C. Wei, S. Vishveshwara, P.M. Gold-

bart, A. Bezryadin, *Science* **304**, 1132 (2004)

[11] L. S. Levitov, A. M. Tsvelik, *Phys. Rev. Lett.* **90**, 016401 (2003); [cond-mat/0205344](https://arxiv.org/abs/cond-mat/0205344)

[12] D.S. Novikov, preprint [cond-mat/0407498](https://arxiv.org/abs/cond-mat/0407498)

[13] D.J. Gross and A. Neveu, *Phys. Rev. D* **10**, 3235 (1974)

[14] Yu.V. Nazarov, D.V. Averin, *Phys. Rev. Lett.* **81**, 653 (1998); R. Klesse, A. Stern, *Phys. Rev. B* **62**, 16912 (2000); M. Pustilnik, E.G. Mishchenko, L.I. Glazman, and A.V. Andreev, *Phys. Rev. Lett.* **91**, 126805 (2003)

[15] S. Frank, P. Poncharal, Z.L. Wang, and W.A. de Heer, *Science* **280**, 1744 (1998); M.J. Biercuk, N. Mason, J. Martin, A. Yacoby, C.M. Marcus, [cond-mat/0406652](https://arxiv.org/abs/cond-mat/0406652); K.A. Matveev, *Phys. Rev. Lett.* **92**, 106801 (2004)